Heliyon 9 (2023) e21032

Contents lists available at ScienceDirect

Heliyon

journal homepage: www.cell.com/heliyon

Anti-inflammatory of disenecionyl *cis*-khellactone in LPS-stimulated RAW264.7 cells and the its inhibitory activity on soluble epoxide hydrolase

Ji Hyeon Park [a,1], Jang Hoon Kim [b,1], Seon Il Jang [a,c,**], Byoung Ok Cho [a,*]

[a] Institute of Health Science, Jeonju University, 303 Cheonjam-ro, Wansan-gu, Jeonju-si, Jeollabuk-do, 55069, Republic of Korea
[b] Department of Herbal Crop Research, National Institute of Horticultural & Herbal Science, RDA, Eumsung, 27709, Republic of Korea
[c] Department of Health Management, Jeonju University, 303 Cheonjam-ro, Wansan-gu, Jeonju-si, Jeollabuk-do, 55069, Republic of Korea

ARTICLE INFO

Keywords:
Peucedanum japonicum thunberg
Disenecionyl *cis*-khellactone
Anti-inflammation
NF-κB
MAPK
Soluble epoxide hydrolase

ABSTRACT

The objective of the present study was to investigate anti-inflammatory effects of disenecionyl *cis*-khellactone (DK) isolated from *Peucedanum japonicum* Thunberg, a traditional edible plant, in RAW264.7 cells stimulated with lipopolysaccharide (LPS). Anti-inflammatory effects of DK were analyzed using various techniques, including NO assay, Western blot analysis, enzyme-linked immunosorbent assay (ELISA), real-time PCR, and immunofluorescence staining. It was revealed that DK reduced the production of pro-inflammatory cytokines including Monocyte chemoattractant protein-1 (MCP-1), Tumor necrosis factor-α (TNF-α), Interleukin 1β (IL-1β), and Interleukin 6 (IL-6) in RAW264.7 cells stimulated with LPS. It was revealed that DK effectively downregulated expression levels of iNOS and COX-2 due to inhibition of NF-κB activation and suppressing the phosphorylation of p38 and jun N-terminal kinase (JNK) mitogen-activated protein kinase (MAPK) phosphorylation. Also, soluble epoxide hydrolase activity and expression were decreased by the proinflammatory inhibitor, DK. Finally, findings of this study suggest that DK isolated from *P. japonicum* might have potential as a therapeutic candidate for inflammatory diseases.

1. Introduction

Peucedanum japonicum Thunberg is a crop cultivated for food consumption in Korea, China, and Japan. In traditional medicine, it has been employed to treat respiratory disorders and seizures. Recent research has explored its possibilities as both an antioxidant and a substance that could help combat obesity [1]. Chemical compositions of *P. japonicum* include several compounds such as rutin, mannithorchromone, polyacetylene, and coumarin. Coumarin, a compound that is abundant in natural products, is well-known for its anti-coagulant, anti-platelet, and anti-cancer properties [2]. In addition, coumarin-based compounds such as isosamidin,

* Corresponding author. Institute of Health Science, Jeonju University, 303 Cheonjam-ro, Wansan-gu, Jeonju-si, Jeollabuk-do, 55069, Republic of Korea.
** Corresponding author. Institute of Health Science, Jeonju University, 303 Cheonjam-ro, Wansan-gu, Jeonju-si, Jeollabuk-do, 55069, Republic of Korea.
E-mail addresses: wlgusliza@naver.com (J.H. Park), oasis5325@gmail.com (J.H. Kim), sonjjang@jj.ac.kr (S.I. Jang), enzyme21@jj.ac.kr (B.O. Cho).
[1] These authors contribute equally to the work.

https://doi.org/10.1016/j.heliyon.2023.e21032
Received 25 July 2023; Received in revised form 12 October 2023; Accepted 13 October 2023
Available online 14 October 2023

peucedanol-7-*O*-*β*-D-glucopyranoside, and disenecionyl *cis*-khellactone (DK, Fig. 1A) have been isolated from *P. japonicum* [3]. Especially, DK has been reported to have anti-diabetic and anti-obesity effects [4].

The human immune system can activate an inflammatory response to protect the body from damage. Inflammation response is a set of protective mechanisms to eliminate threats, promote tissue repair, and restore physiological equilibrium. Nonetheless, studies have shown that the transition of inflammation to a chronic or dysregulated state is associated with a wide range of diseases, from autoimmune diseases to cardiovascular diseases, chronic respiratory diseases, neurodegenerative diseases and malignancies [5]. Macrophages play a key role in controlling immune reactions and significantly affect the development of inflammatory conditions. Macrophages can recognize stimuli through toll-like receptors (TLRs) and activate signaling pathways such as mitogen-activated protein kinase (MAPK) and nuclear factor kappa-light-chain-enhancer of activated B cells (NF-κB). MAPKs are pivotal gene-regulatory proteins that play a central role in cellular signaling networks. These proteins, including p38, jun N-terminal kinase (JNK), and extracellular signal-regulated kinase (ERK), function as signal transducers by detecting various external stimuli, such as growth factors or changes in the alkaline environment. They phosphorylate and activate the respective p38, JNK, and ERK pathways, thereby relaying diverse signals. MAPKs are reported to regulate processes like cell survival, growth, differentiation, and inflammatory responses [6]. They can induce the production of NO, other inflammatory factors, and cytokines [7].

Nitric oxide synthase (NOS) includes neuronal NOS (nNOS), endothelial NOS (eNOS), and inducible NOS (iNOS) types. Among them, iNOS produces a large amount of NO. It is involved in immune responses [8]. Tumor necrosis factor-α (TNF-α) is a crucial cytokine that regulates inflammatory immune response. It has the ability to produce interleukin-1 (IL-1) and interleukin-6 (IL-6) [9]. Prostaglandin-endoperoxide synthase 2 (PGE_2) produced by cyclooxygenase-2 (COX-2) and monocyte chemoattractant protein-1 (MCP-1) are typical pro-inflammatory cytokines that can regulate immune responses [10]. In particular, MCP-1 can attract immune cells to inflammatory sites [11]. When signal transduction mechanisms of macrophages are activated by Lipopolysaccharide (LPS) stimulation, the production of various inflammation-related factors and cytokines is increased, causing various diseases.

Soluble epoxide hydrolase (sEH) is an enzyme belonging α/β-hydrolase family that converts epoxyeiocosanoids acids (EETs) to dihydroxyeicosatrienoic acids (DHETs) [12]. Especially, EETs have the property of anti-inflammation by inhibiting NF-κB activity and TNF-α-induced vascular cell adhesion protein 1 (VCAM-1) expression [13]. Among them, it revealed obviously that 11,12-EET suppresses LPS-induced COX-2 expression and prostaglandin E2 production [14]. Especially, sEH is highly expressed in LPS-stimulated lung macrophages [13]. Therefore, sEH has been known as a target for anti-inflammatory treatment, and researchers are continuously striving to develop natural inhibitors to replace urea-type sEH inhibitors [15,16].

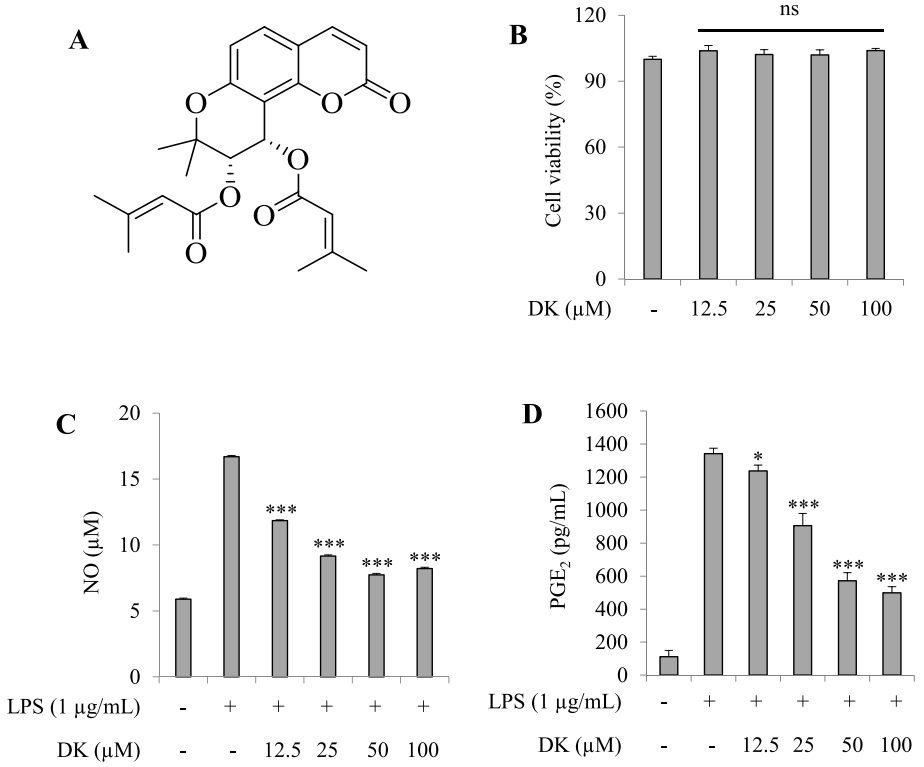

Fig. 1. The structure of DK (A) and effects of DK on cell viability and inhibition of NO, PGE_2 production in LPS-stimulated RAW264.7 cells. Cell viability (0–100 μM) was assessed by WST-8 assay (B). The cells were pre-treated with DK (12.5–100 μM) for 1 h, followed by stimulation with LPS (1 μg/mL) and incubated at 37 °C with 5 % CO_2 for 24 h. Subsequently, the supernatant was obtained. NO production was performed by Griess reagent assay (C) and PGE_2 production confirmed by ELISA assay (D). Each bar represents the mean ± SD. Different small case letters indicate significant differences at *$p < 0.05$, **$p < 0.01$, ***$p < 0.001$ vs. LPS alone, ns > 0.05 vs. control.

Recently, some studies are being actively conducted to effectively control proinflammatory cytokines [17,18]. Despite various pharmacological properties of *P. japonicum* and its constituent compounds have been reported [19,20] anti-inflammatory effects of DK are still largely unknown. Therefore, the objective of this study is to positively regulate the expression of proinflammatory cytokines in LPS-stimulated RAW264.7 cells and an anti-inflammatory direction by isolated DK, and to inhibit sEH activity and expression by DK.

2. Material and methods

2.1. Materials

DK was obtained from Dr. J.H Kim of Department of Herbal Crop Research, National Institute of Horticultural and Herbal Science. Dulbecco's modified Eagle medium (DMEM) and fetal bovine serum were bought from Gibco (Grand Island, NY, USA). Quanti-Max™ WST-8 Cell Viability Assay Kit was bought from Biomax (Guri-si, Gyeonggi-do, Korea). Lipopolysaccharides (LPS) and Griess reagent were purchased from Sigma-Aldrich (St. Louis, MO, USA). PGE_2, IL-1β, TNF-α, IL-6, and MCP-1 ELISA kit were bought from R&D Systems (Minneapolis, MN, USA). COX-2 antibody was purchased from Cayman Chemical (Ann Arbor, MI, USA). ProLong® Gold Antifade Reagent with DAPI (8961S) and antibodies targeting p-Erk1/2 (#9101, rabbit Polyclonal), total Erk1/2 (#9102, rabbit Polyclonal) were obtained form Cell signaling technology, Inc. (Danvers, MA, USA). And JNK (sc-7345, mouse monoclonal), p-JNK (sc-293136, mouse monoclonal), p38 (sc-81621, mouse monoclonal), p-p38 (SC-166182, mouse monoclonal) NF-κB (sc-8008, mouse monoclonal), p-NF-κB (sc-136548, mouse monoclonal), HO-1 (sc-136960, mouse monoclonal), soluble epoxide hydrolase (sEH, sc-166961, mouse monoclonal) and actin (sc-8432, mouse monoclonal), m-IgGκ BP-HRP (sc-516102, mouse) were obtained from Santa Cruz Biotechnology, Inc. (Santa Cruz, CA, USA). Goat anti-rabbit IgG (H + L) Secondary Antibody, HRP (#31460, goat anti-rabbit) Alexa Fluor 488-conjugated goat anti-mouse IgG secondary antibody(A-11001) was purchased from Invitrogen, Inc.(Waltham, MA, USA). Human recombinant soluble epoxide hydrolase (sEH, 10011669), cyano-(6-methoxynaphthalen-2-yl)methyl] 2-(3-phenyloxiran-2-yl)acetate (PHOME, 10009134), and 12-(3-((3s,5s,7s)-adamantan-1-yl)ureido)dodecanoic acid (AUDA, 10007972) were purchased from Cayman Chemical (Ann Arbor, MI, USA).

2.2. Cell culture

RAW264.7 cell line was obtained from ATCC (Manassas, VA, USA). Cells were cultured in DMEM supplemented with 10 % FBS and 1 % penicillin/streptomycin. Cells were subcultured every 2 days and maintained in a 37 °C, 5 % CO_2 incubator. All experiments were conducted using the RAW264.7 cell line at passages 9–12.

2.3. Cell viability

RAW264.7 cells were seeded in a 96-well plate at a density of 2×10^5 cells/mL, with 100 μL per well and cultured for 24 h in an incubator maintained at 37 °C, 5 % CO_2. Cells were treated with DK (12.5–100 μM) for 20 h. Thereafter, 10 μL of Quanti-Max™ WST-8 Cell Viability Assay Kit was added into each well. After 4 h of incubation, absorbance was measured at wavelength of 450 nm using a spectrophotometer (SUNRISE, Tecann Group, Ltd.).

2.4. Nitric oxide assay

RAW264.7 cells were seeded in a 96-well plate at a density of 2×10^5 cells/mL, with 100 μL per well and cultured for 24 h in an incubator maintained at 37 °C, 5 % CO_2. Prior to LPS (1 μg/mL) stimulation, cells were pretreated with DK (12.5–100 μM) for 1 h, followed by continued culture for an additional 24 h. After incubation, 100 μL of Griess reagent was added to 100 μL of the supernatant in the 96-well plate. After 15 min of incubation, the absorbance was measured at wavelength of 540 nm using a spectrophotometer (SUNRISE, Tecann Group, Ltd.).

2.5. Enzyme-linked immunosorbent assay

RAW264.7 cells were seeded in a 60 mm cell culture dishes at a density of 2×10^5 cells/mL, with 4 mL per well and cultured for 24 h in an incubator maintained at 37 °C, 5 % CO_2. These cells were pretreated with DK (12.5–100 μM or 50 and 100 μM) for 1 h, followed by continued culture for an additional 20 h with LPS (1 μg/mL) stimulation, after which supernatants were collected. Concentrations of PGE_2, IL-1 β, TNF-α, IL-6, and MCP-1 in the supernatants were measured using ELISA kits according to the manufacturer's protocol.

2.6. RNA extraction and RT-PCR

RAW264.7 cells were seeded in a 60 mm cell culture dishes at a density of 2×10^5 cells/mL, with 4 mL per well and cultured for 24 h in an incubator maintained at 37 °C, 5 % CO_2. These cells were pretreated with DK (50 and 100 μM) for 1 h, followed by LPS (1 μg/mL) stimulation for 3 h. Total RNAs were extracted from cells using an RNA-spin™ Total RNA Extraction Kit (iNtRON Biotechnology, Seungnam-si, Gyeonggi-do, Korea) and reverse transcribed into cDNAs using an iScript™ cDNA Synthesis Kit (1708891) and a T100TM Thermal Cycler (Bio-Rad, Hercules, CA, USA). Resulting cDNAs were amplified using a SYBR (TOYOBO, Osaka, Japan) kit. Real-time PCR was performed using a StepOne Real-Time PCR system (Thermo Fisher Scientific, Waltham, MA, USA) and gene

expression levels were quantified. Primers used for PCR analysis were: TNF-α: 5′-CATGTGCTCCTCACCCACAC-3' (forward) and 5′-ATGGGCTCATACCAGGGCTT-3' (reverse), iNOS: 5′-CGGAGTGACGGCAAACATGA-3' (forward) and 5′-TTCCAGCCTAGGTCGATGCA-3' (reverse), GAPDH: 5′-GGCTACACTGAGGACCAGGT-3' (forward) and 5′-TCCACCACCCTGTTGCTGTA-3' (reverse). The thermal profile included 95 °C for 5 min and 30 cycles of amplification at 95 °C for 30 s and 60 °C for 30 s. Expression levels were normalized to GAPDH using the $2^{-}\Delta\Delta Ct$ method. All protocols followed the manufacturer's instructions without any modifications.

2.7. Protein extraction and western blot

RAW264.7 cells were seeded in a 60 mm cell culture dishes at a density of 2×10^5 cells/mL, with 4 mL per well and cultured for 24 h in an incubator maintained at 37 °C, 5 % CO_2. These cells were pretreated with DK (12.5–100 μM or 50 and 100 μM). After 1 h, cells were stimulated with LPS (1 μg/mL) for 30 min or 24 h. Next, protein extraction was performed with RIPA buffer (with 1 % protease and phosphatase inhibitors) and quantified by the Bradford's method. The process of separating and analyzing proteins involved the following steps: (1) separation of proteins with 7.5 % or 10 % polyacrylamide gels at 100 V for 1 h, (2) transfer of proteins from the gel to PVDF membranes at 100 V for 1 h and blocking with 5 % skim milk for 1 h, (3) after washing step with TBST, incubation of membranes with primary antibodies (COX-2, 1:2000; HO-1, 1:200; iNOS, 1:5000; p-p38, 1:500; p-38, 1:500; p-ERK, 1:1000; ERK, 1:1000; p-JNK, 1:500; JNK, 1:500; β-actin, 1:2000; p-NF-κB, 1:500; NF-κB, 1:500) overnight at 4 °C, (4) washing membranes three times with TBST solution for 10 min, (5) incubation of membranes with either mouse or rabbit HRP-conjugated secondary antibodies (1:5000) in 5 % skim milk for 2 h at room temperature, (6) washing membranes three times with TBST solution for 10 min, and (7) developing membranes with an EZ-western Lumi Pico Alph reagent, capturing images of membranes using an imaging system (Alliance version 15.11; UVITEC), and analyzing band densities using ImageJ program (National Institute of Health, Bethesda, MD, USA).

2.8. Immunofluorescence staining

RAW264.7 cells were seeded in a 4-well cell culture slides at a density of 2×10^5 cells/mL, with 250 μL per well and cultured for 24 h in an incubator maintained at 37 °C, 5 % CO_2. These cells were then treated with DK (50 or 100 μM) for 1 h followed by stimulation with LPS (1 μg/mL) for 30 min. After incubation, cells were fixed with 4 % paraformaldehyde for 1 h and washed three times with PBS. Subsequently, cells were incubated with 1 % BSA for 1 h and then incubated with primary antibody (p-NF-κB, 1:200; NF-κB, 1:200) overnight at 4 °C. Next, cells were washed twice with PBS and incubated with Alexa Fluor 488-conjugated goat anti-mouse IgG secondary antibody (1:2000) in 1 % BSA for 1 h at room temperature. After washing three times with PBS, cells were mounted with DAPI and images were captured using a AXIOSKOP 45 14 85 fluorescence microscope (ZEISS microscope, Oberkochen, Germany). All procedures were performed according to the manufacturer's instructions without modification.

2.9. sEH activity assay and molecular simulation

Enzymatic assays, and molecular docking and dynamics studies were performed according to a previously described method with some modifications [21]. sEH in 0.2 mM tris-HCl (pH 7.0) containing 0.1 % BSA buffer was mixed with 200 μL of DK in methanol. When 50 μL PHOME in buffer is added to the mixture, the enzyme catalytic reaction starts. The results of the reaction were measured using a fluorescence photometer (excitiation: 330 nm, emission: 465 nm).

Molecular docking between sEH (PDB id: 3ANS) and DK was performed using Autodock 4.2 (La Jolla, CA, USA) and Chem 3D (CambridgeSoft, Cambridge, MA, USA) programs. After setting up the grid ($60 \times 60 \times 60$ at 0.375 Å) including the active site, flexible ligand docking was performed (Lamarckian genetic algorithm). Molecular dynamics was performed using Gromacs 4.6.5 program (Uppsala University, Uppsala, Sweden). sEH and DKwas charged by a CHARMM all-atom force field and CHARMM360ff, respectively. The complex was dissolved in a cubic box with H_2O containing six sodium ions. The complex was energy stabilization (a maximal force 10 kJ/mol), and NVT and NPT equlibrations, and then molecular dynamics was performed. The results were represented visually as SigmaPlot (San Jose, CA, USA) and Chimera (San Francisco, CA, USA).

2.10. Statistical analysis

Data are presented as mean ± standard deviation and statistical analysis was conducted using the SPSS software (SPSS Inc, Chicago, IL, USA). One-way analysis of variance (ANOVA) followed by Turkey's test to determine any significant differences among groups. A *p*-value of less than 0.01, 0.05 or 0.001 was considered statistically significant. All experiments were performed in triplicate.

3. Results

3.1. DK suppresses NO and PGE_2 production in LPS-stimulated RAW264.7 cells

DK was isolated with silica and C-18 column chromatographies from the ethanol extract of *P. japonicum*. This chemical structure was elucidated by analyzing Mass, ^1H and ^{13}C NMR spectra (Figs. S1–S3). Inhibitory effects of DK on NO and PGE_2 production in LPS-stimulated RAW264.7 cells were investigated. First, as a result of measuring the amount of NO produced after determining the concentration of DK to be used to treat cells based on cell viability (Fig. 1B), When the amount of NO production increased by LPS was treated with DK, NO production was shown to be suppressed starting from 12.5 μM ($P < 0.001$) (Fig. 1C). In addition, it was confirmed

that the amount of PGE_2 produced increased by LPS was decreased by DK in a concentration-dependent manner starting from 25 μM ($P < 0.01$) (Fig. 1D).

3.2. DK suppresses iNOS, COX-2 and increased HO-1 expression in LPS-stimulated RAW264.7 cells

Western blot analysis was performed for RAW264.7 cells stimulated with LPS to assess the effect of DK on the expression of iNOS, COX-2 and HO-1 (Fig. 2A–D). As shown in Fig. 2B, when treated with DK at concentrations ranging from 12.5 μM to 100 μM, there was a significant reduction in iNOS expression of over 40 % starting at 12.5 μM compared to the LPS-treated group. Furthermore, a concentration-dependent trend of decreasing iNOS expression was observed, commencing at 12.5 μM ($p < 0.001$). Fig. 2C shows that the expression of COX-2, which was increased by LPS, was reduced by more than 35 % starting from 25 μM of DK, and showed a tendency to gradually decrease in a concentration-dependent manner ($p < 0.001$). On the other hand, Fig. 2D shows that HO-1 expression in the DK-treated group increased by more than 642 % from 12.5 μM treatment compared to the LPS-treated group ($p < 0.001$).

3.3. DK suppresses TNF-α and iNOS mRNA expression in LPS-stimulated RAW264.7 cells

Inhibitory effects of DK on TNF-α and iNOS gene expression in LPS-stimulated RAW264.7 were investigated. As shown in Fig. 3A, TNF-α mRNA levels in DK-treated groups at 50 and 100 μM were reduced by 36.0 % and 21.4 % ($p < 0.001$), respectively, compared to that in the LPS-treated group. As shown in Fig. 3B, mRNA levels of iNOS in DK-treated groups at 50 and 100 μM were reduced by 58.7 % and 44.6 % ($p < 0.001$), respectively, compared to that in the LPS-treated group.

3.4. DK suppresses expression of pro-inflammatory cytokines in LPS-stimulated RAW264.7 cells

Inhibitory effects of DK on expression of IL-1β, TNF-α, IL-6, and MCP-1 in RAW264.7 cells stimulated with LPS were investigated. As depicted in Fig. 4A–D, the expression of IL-1β in DK-treated groups at concentrations of 25 μM, 50 μM, and 100 μM was reduced by 21.6 %, 50.4 %, and 57.6 %, respectively, compared to that in the LPS-treated group ($p < 0.001$) (Fig. 4A). Similarly, as shown, the expression of TNF-α in DK-treated groups at concentrations of 25 μM, 50 μM, and 100 μM was reduced by 10.8 %, 58.6 %, and 71.1 %, respectively, compared to that in the LPS-treated group ($p < 0.001$) (Fig. 4B). Furthermore, the expression of IL-6 also decreased in the DK-treated groups at concentrations of 25 μM, 50 μM, and 100 μM, with reduction percentages of 23.1 %, 51.6 %, and 67.2 %,

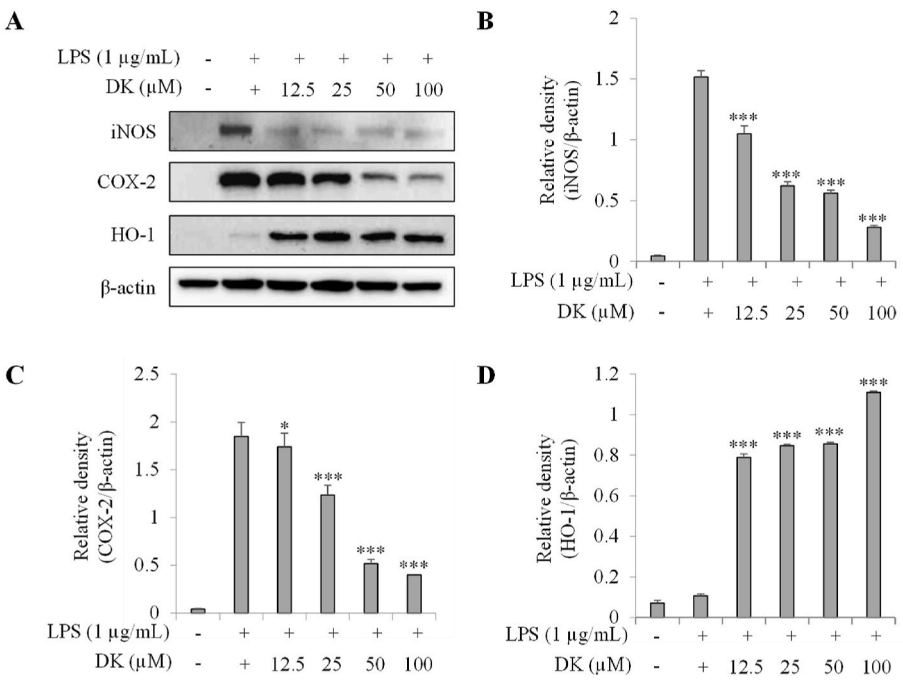

Fig. 2. Inhibitory effect of DK on iNOS and COX-2 and increased expression of HO-1 in LPS-stimulated RAW264.7 cells. Cells were pretreated with DK (12.5–100 μM) for 1 h and then stimulated with LPS (1 μg/mL) and incubated at 37 °C with 5 % CO_2 for 24 h. Expression levels of iNOS, COX-2 and HO-1 (A) were measured by Western blot. Relative densities of iNOS (B), COX-2 (C) and HO-1 (D) were calculated using ImageJ. Each bar represents mean ± SD (n = 3). Different lowercase letters indicate significant differences at *$p < 0.05$, **$p < 0.01$, ***$p < 0.001$ vs. LPS alone. Refer to Supplementary Figs. S1–4 for uncropped version of Fig. 2A.

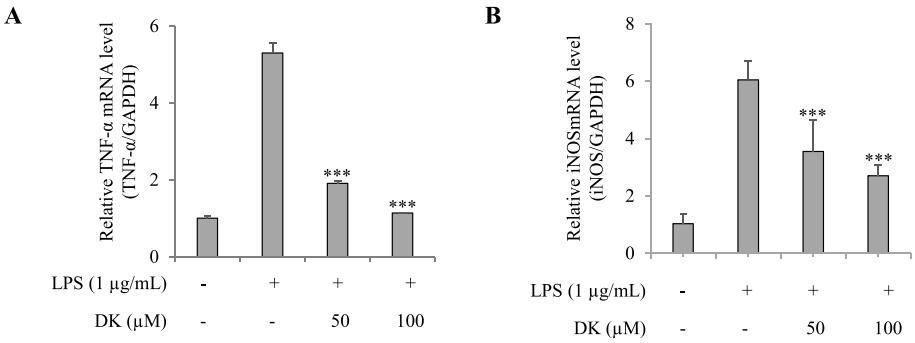

Fig. 3. Inhibitory effect of DK on TNF-α (A) and iNOS (B) mRNA levels in LPS-stimulated RAW264.7 cells. Cells were pretreated with DK (50, 100 μM) hours and then stimulated with LPS (1 μg/mL) and incubated at 37 °C with 5 % CO_2 for 24 h mRNA expression levels of TNF-α (A) and iNOS (B) were measured by real-time PCR. Each bar represents mean ± SD (n = 3). Different lowercase letters indicate significant differences at *p < 0.05, **p < 0.01, ***p < 0.001 vs. LPS alone.

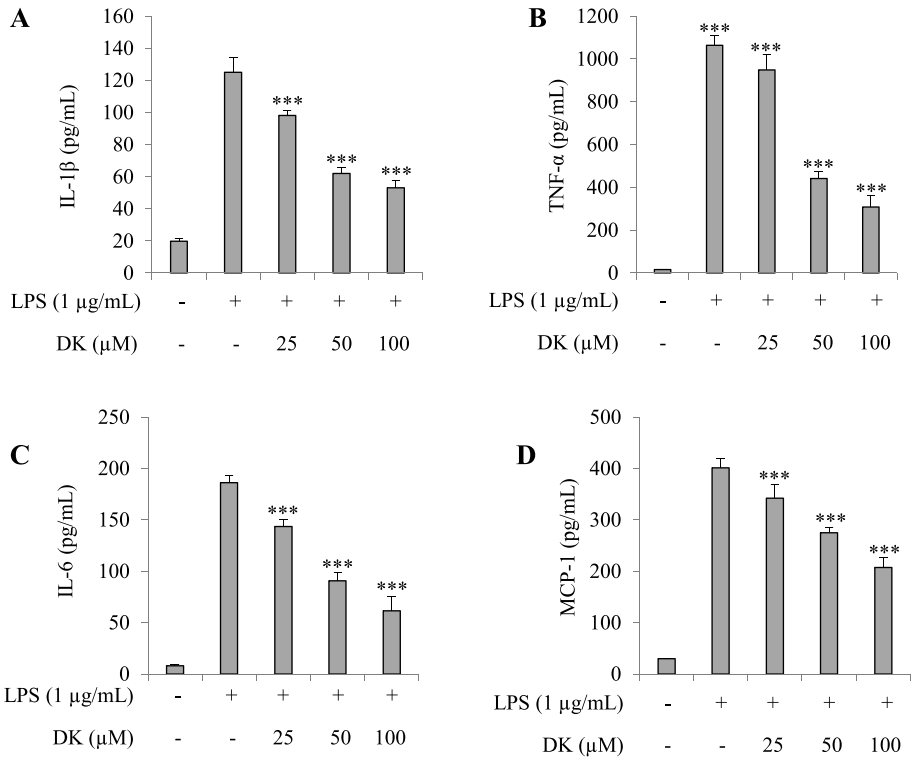

Fig. 4. Inhibitory effect of DK on pro-inflammatory cytokines in LPS-stimulated RAW264.7 cells. The cells were pre-treated with DK (50, 100 μM) for 1 h, followed by stimulation with LPS (1 μg/mL) and incubated at 37 °C with 5 % CO_2 for 24 h. Subsequently, supernatant was obtained. Expression of IL-1β (A), TNF-α (B), IL-6 (C) and MCP-1 (D) were measured by ELISA assay. Each bar represents mean ± SD (n = 3). Different lowercase letters indicate significant differences at *p < 0.05, **p < 0.01, ***p < 0.001 vs. LPS alone.

respectively, compared to the LPS-treated group (p < 0.001) (Fig. 4C). Similarly, the expression of MCP-1 exhibited comparable results, with reductions of more than 14.9 %, 31.7 %, and 48.4 % in the 25 μM, 50 μM, and 100 μM DK-treated groups, respectively, compared to the LPS-treated group (p < 0.001) (Fig. 4D).

3.5. DK suppresses phosphorylation of p-38 and JNK in LPS-stimulated RAW264.7 cells

To investigate the mechanism of DK's inhibition on inflammation, its inhibitory effect on MAPK phosphorylation was evaluated in LPS-stimulated RAW264.7 cells. Fig. 5A–D showed that the phosphorylation levels of p-38 and JNK increased in the LPS-treated group. On the other hand, in groups treated with 50 μM and 100 μM concentrations of DK, the phosphorylation levels of p-38 decreased by 27 % and 42 %, respectively (p < 0.001) (Fig. 5B). A similar trend was observed in the phosphorylation levels of JNK (Fig. 4D). The

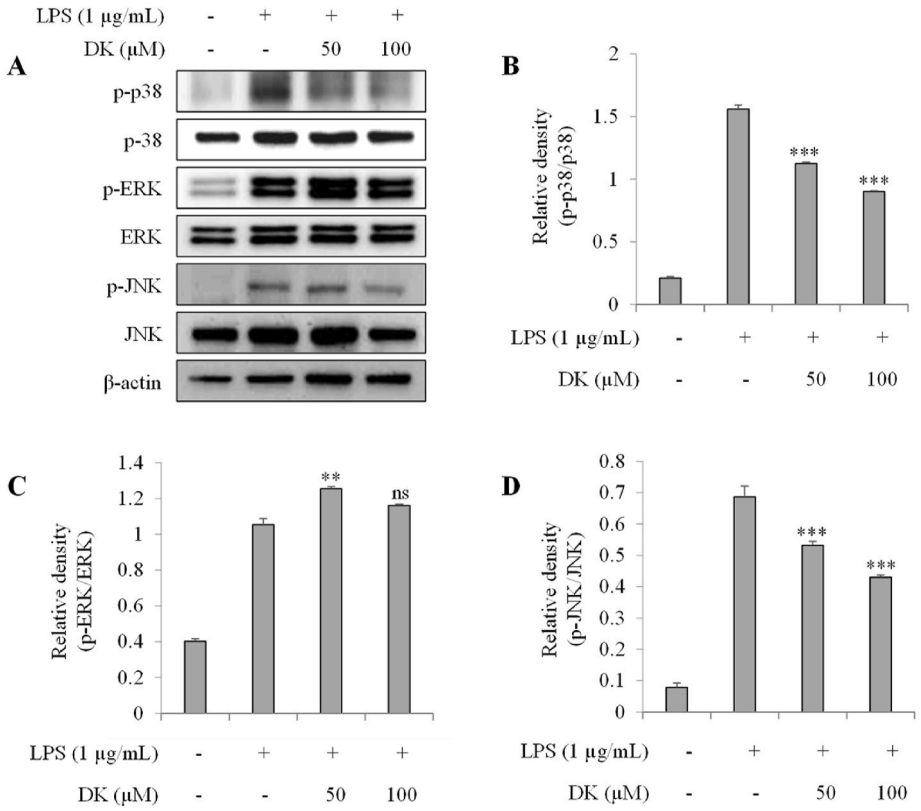

Fig. 5. Inhibitory effect of DK on MAPK activation in LPS-stimulated RAW264.7 cells. Cells were pretreated with DK (50, 100 μM) for 1 h and then stimulated with LPS (1 μg/mL) and incubated at 37 °C with 5 % CO_2 for 30 min. Phosphorylation level of MAPKs (A) were measured by Western blot. Relative densities of p-38 (B), ERK (C), JNK (D) were calculated using ImageJ. Each bar represents mean ± SD (n = 3). Different lowercase letters indicate significant differences at *p < 0.05, **p < 0.01, ***p < 0.001, ns > 0.05 vs. LPS alone. Refer to Supplementary Figs. S5–11 for uncropped version of Fig. 5A.

increase in JNK phosphorylation seen in the LPS-treated group was reduced by 22 % and 37 % in the DK 50 and 100 μM treated groups, respectively ($p < 0.001$). But ERK phosphorylation was not decreased by DK treatment (Fig. 5C).

3.6. DK suppresses phosphorylation of NF-κB in LPS-stimulated RAW264.7 cells

To investigate the mechanism of DK's inhibition on inflammation, the inhibitory effect on NF-κB phosphorylation in LPS-stimulated RAW264.7 was evaluated by Western blot (Fig. 6A and B) and immunofluorescence staining (Fig. 6C and D). The phosphorylation of NF-κB, which increased due to LPS stimulation, was significantly reduced by 71 % and 77 % in the DK 50 and 100 μM treatment groups, respectively ($p < 0.001$) (Fig. 6A and B). Furthermore, phosphorylated NF-κB translocated to the nucleus. However, the NF-κB translocation potential was partially restored, showing increases of 4 % and 26 % in the 50 and 100 μM DK treatment groups, respectively ($p < 0.01$) (Fig. 6C and D).

3.7. Inhibitory activity of DK on sEH

DK was tested for inhibitory activities toward sEH catalytic reaction and expression *in vitro*. As showed in Fig. 7A and Table 1, it is obvious that the degree of inhibition in the reaction is reduced by increasing DK concentration. As the result, the compound was confirmed to have the property with IC_{50} value of 1.7 ± 0.4 μM (Fig. 7A). Positive control was used as AUDA. Moreover, the potential inhibitor was bound into sEH as competitive mode with k_i value of 1.1 ± 0.7 μM by lineweaver burk and dixon plots (Fig. 7B and C). Moreover, the sEH expression level in LPS-stimulated RAW264.7 cells was found to be increased compared to the normal control group. However, in a dose-dependent manner, the sEH expression level decreased by 7 %, 76 %, and 96 % in LPS-stimulated RAW264.7 cells treated with 25, 50, and 100 μM of DK, respectively ($p < 0.05$) (Fig. 7D).

3.8. Predicted binding of DK with sEH

DK was simulated using autodock 4.2 and gromacs 4.6.2 packages based on computational chemistry theory to predict binding at

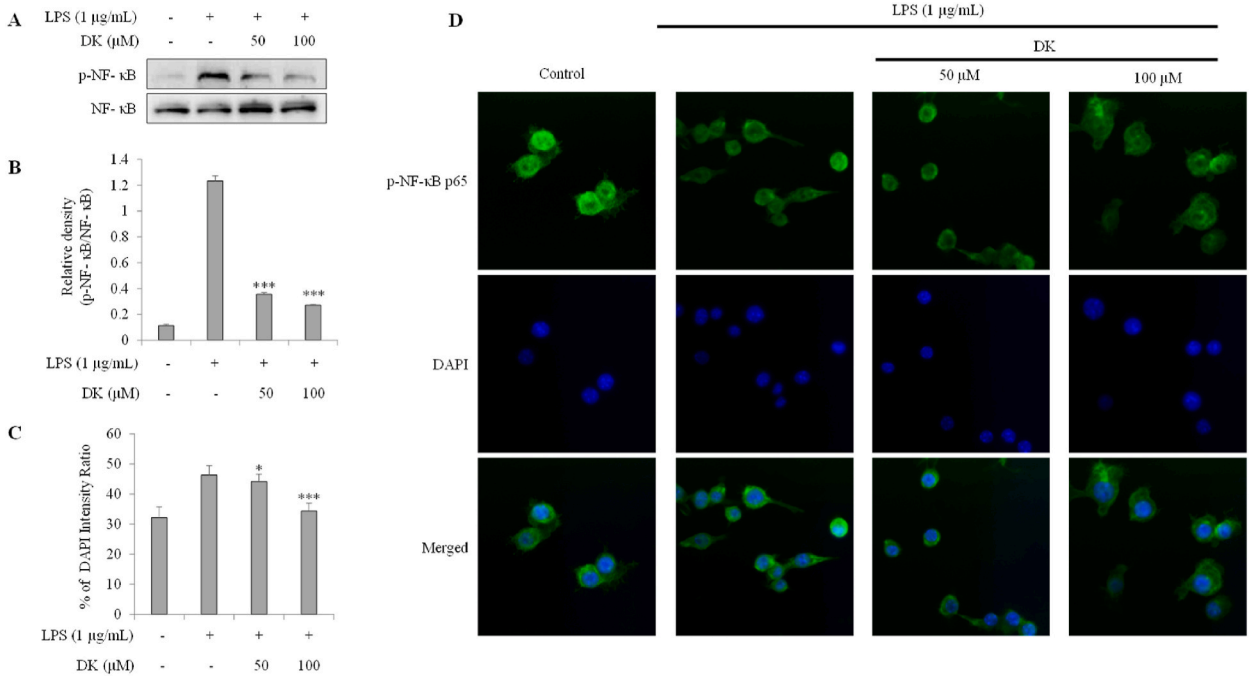

Fig. 6. Inhibitory effect of DK on NF-κB phosphorylation and nuclear translocation in LPS- stimulated RAW264.7 cells. Cells were pretreated with DK (50, 100 μM) for 1 h and then stimulated with LPS (1 μg/mL) and incubated at 37 °C with 5 % CO_2 for 30 min. Expression levels of NF- κB (A) was measured by Western blot. Relative densities of NF- κB (B). Translocation of NF- κB intensity ratio (C) was measured by immunofluorescence (D). There were calculated using ImageJ. Each bar represents mean ± SD (n = 3). Different lowercase letters indicate significant differences at *p < 0.05, **p < 0.01, ***p < 0.001 vs. LPS alone. Refer to Supplementary Figs. S12–13 for uncropped version of Fig. 6A.

the sEH active site (based on competitive inhibitor). As indicated in Fig. 8A–B, Table 1, DK made the hydrogen bond at 2.93 Å distance to Gln284 with −9.8 kcal/mol autodock score. The most stable state of ligand docked into receptor was performed molecular dynamics study with CHARMM36 force field. As the result, the complex was stable in the active site for 30 ns and exhibited a flexible movement with about -1.32×10^6 kJ/mol potential energy (Fig. 8C–D). The protein-based root-mean-square deviation (RMSD) and root-mean square deviation (RMSF) values of sEH by DK were within - 0.30 nm (Fig. 8E–F). Furthermore, DK maintained 0–1 hydrogen bonds with amino acids (Fig. 8G).

4. Discussion

An inflammatory reaction is a typical innate immune response that protects the body from external stimuli [22]. Activation of macrophages is the main cause of an immune response, and LPS is a typical substance that causes a macrophage-mediated inflammatory response [23]. Several studies have shown that NO, PGE_2, pro-inflammatory cytokines, and other inflammation-related factors increase in RAW264.7 cells (rodent-derived macrophages) when they are stimulated with LPS [24]. iNOS produce NO, a pro-inflammatory mediator, and COX-2 is an enzyme expressed by cytokine or LPS in macrophages to play an important role in converting arachidonic acid into PGE_2, an inflammatory mediator [25,26]. Additionally, sEH serves to lower the concentration of EETs which have anti-inflammatory activity by hydrolyzing those [12,13]. Therefore, the downregulation of COX-2 and iNOS expression by natural components might inhibit the generation of PGE_2 and NO, and the perseveration of EETs level by inhibiting sEH activity and expression might also soften the inflammation.

Accordingly, the present study revealed that DK isolated from roots of *P. japonicum* significantly downregulated NO and PGE_2 of which the level was increased due to LPS in RAW264.7 cells. This might be because DK inhibited the expression of COX-2 and iNOS. IL-1β, TNF-α, IL-6, and MCP-1 are known as pro-inflammatory cytokines expressed when macrophages are activated by inflammation [27]. Many previous studies have reported that inhibiting this is useful for regulating inflammation [28,29]. Our study findings showed that DK reduced the expression of IL-1β, TNF-α, IL-6, and MCP-1.

The generation of pro-inflammatory cytokines is related to the activation of MAPK and NF-κB. MAPK is a central signaling pathway that responds to various extracellular stimuli and is activated by kinase cascade to cause the phosphorylation of protein. It regulates various cellular processes, among which it is closely related also to inflammation responses [30]. MAPK is classified into ERK, JNK, and p38. ERK is activated mainly by mitotic stimuli such as growth factors or hormones while JNK and p38 are activated by stress stimuli [31].

NF-κB is a transcription factor involved in the mechanism of inflammation and the activation of abnormal NF-κB is known to cause various immunity-related diseases [32,33]. NF-κB responds to various stimuli and a study has shown that activation of NF-κB in

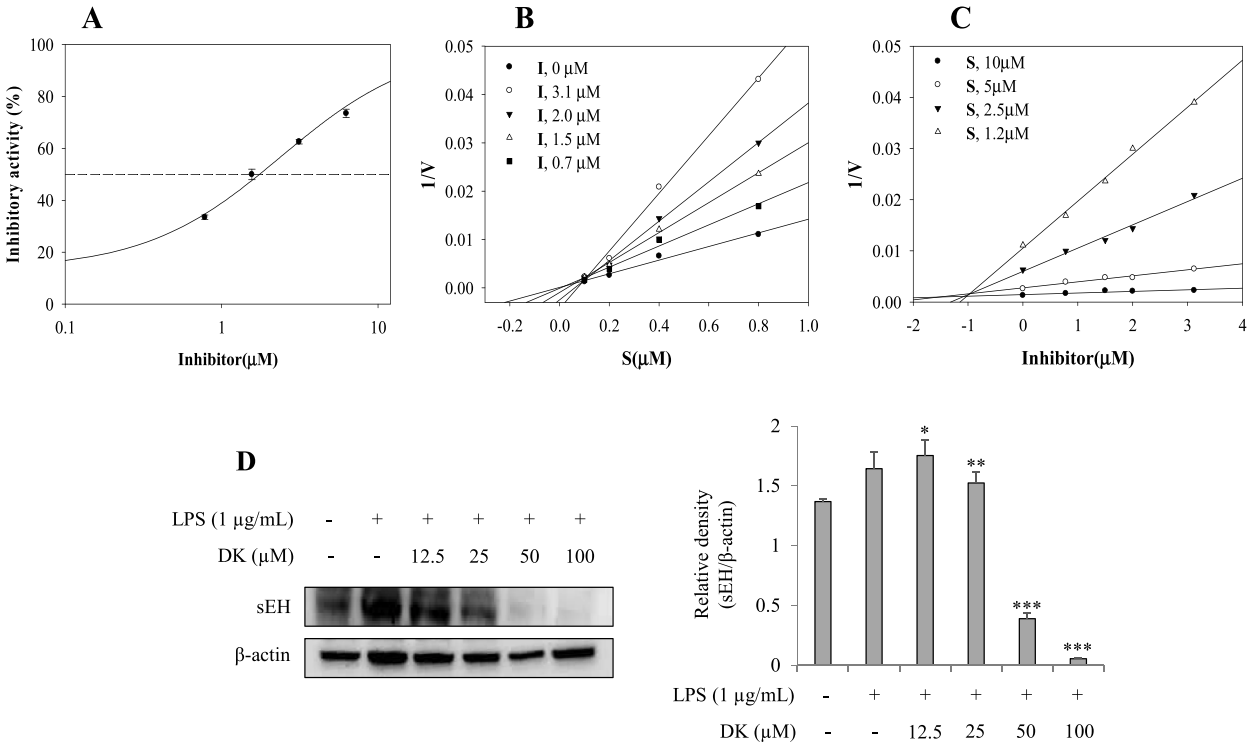

Fig. 7. The inhibitory activity (A), lineweaver burk (B) and Dixon (C) plots of inhibitor on sEH. The inhibitory activity of sEH expression in LPS-stimulated RAW264.7 cells by DK (D). Cells were pretreated with DK (12.5–100 μM) for 1 h and then stimulated with LPS (1 μg/mL) for 24 h. Expression levels of sEH were measured by Western blot. Relative density of sEH was calculated using ImageJ. Each bar represents mean ± SD (n = 3). Different lowercase letters indicate significant differences at *p < 0.05, **p < 0.01, ***p < 0.001 vs. LPS alone. Refer to Supplementary Figs. S14–15 for uncropped version of Fig. 7D.

Table 1
The inhibitory activity, kinetics, and molecular docking of inhibitor with sEH.

	IC_{50}(μM)[a]	Binding Mode(k_i, μM)	Autodock score(kcal/mol) hydrogen bonds
DK	1.7 ± 0.4	1.1 ± 0.7	−9.8; Gln384(2.93)
AUDA[b]	21.2 ± 0.3 nM		

[a] All compound examined in a set of triplicated experiment.
[b] Positive control.

immune cells stimulated by LPS involves expression of inflammatory cytokines [34]. NF-κB combined with IκB exists in the cytoplasm and, when IκB is phosphorylated as a result of IKK activation by a stimulus, NF-κB moves to the nucleus in an activated state to transcribe various inflammatory cytokines [35]. Therefore, we investigated the activation of MAPK and NF-κB signaling pathways to study DK's mechanism of inhibiting pro-inflammation cytokines and inflammatory mediators. The result showed that DK significantly inhibited the phosphorylation of JNK and p38. Such a result suggests that DK can inhibit inflammatory responses by regulating MAPK's JNK and p38 pathways. In addition, DK inhibited the phosphorylation and nuclear translocation of NF-κB. Findings of the present study suggest that the anti-inflammation effect of DK is due to inhibition of MAPK and NF-κB signaling pathways.

DK inhibited the catalytic reaction and expression of sEH at the same time. For this reason, it is believed that DK will have an anti-inflammatory effect by maintaining the concentration of EETs and exerting an inhibitory effect on the expression of inflammatory cytokines. It was unveiled that the inhibitor inhibits the enzyme activity by stably binding to the active site of sEH. However, it can be confirmed that the hydrogen bonding strength is very low in their flexible bonding state, which is probably because the two prenyl groups of DK play a role in hindering hydrogen bonding with amino acids.

5. Conclusion

In conclusion, DK increased the expression of HO-1 in RAW264.7 cells stimulated by LPS and inhibited the generation of NO, iNOS, COX-2, and other inflammatory mediators including PGE_2, TNF-α, IL-6, IL1-β, and MCP-1. It was thought that inflammatory mediators

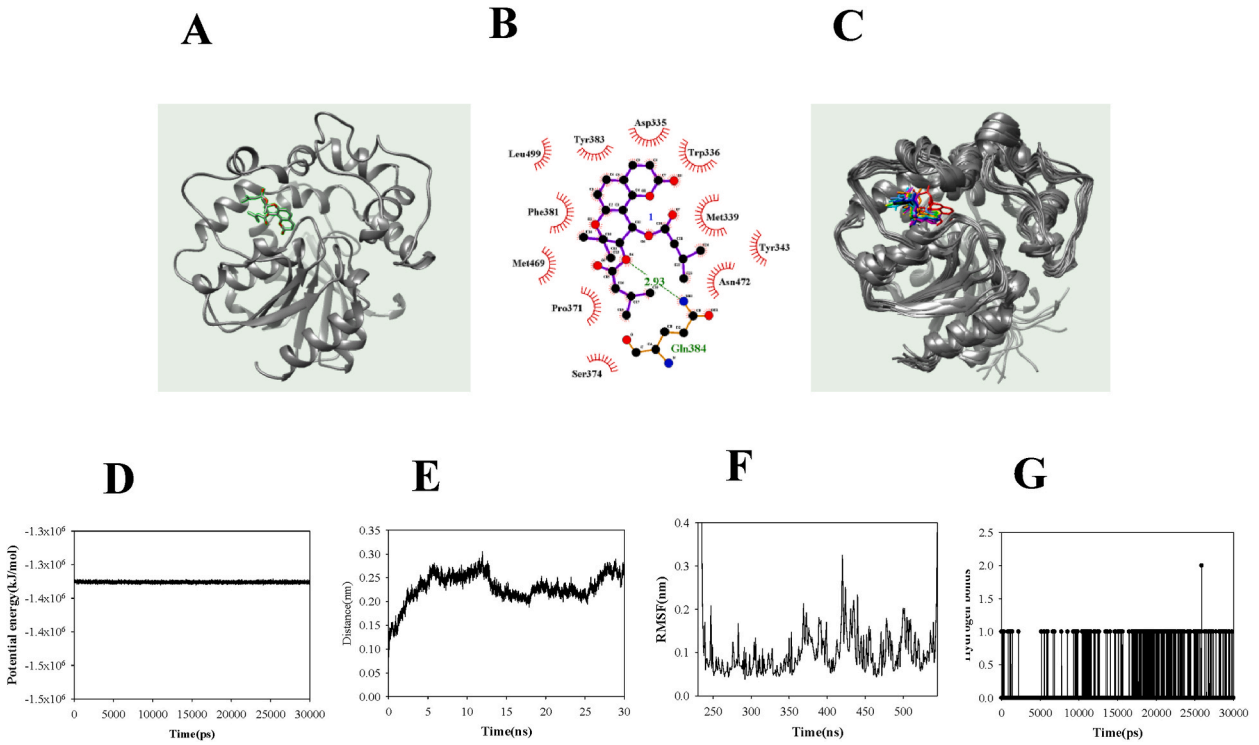

Fig. 8. The best docking position (A) and hydrogen bonds (B) of inhibitor. The superpositions of sEH with inhibitor for the simulation time (red: 0ns, orange: 3ns, yellow: 6ns, green: 9ns, cyan: 12ns, blue: 15ns, conflower blue: 18ns, purple: 21ns, hot pink: 24ns, magenta:27ns, black: 30ns) (C), The RMSD (D), RMSF (E), potential energy (F), and hydrogen bond numbers (G) of the simulation calculated during 30 ns.

were regulated by inhibition of MAPK and NF-κB. Additionally, the potential inhibitor was confirmed to show the effects on the inhibition of sEH activity and expression. Taken together, findings of the present study suggest that DK might be a candidate medicine for treating inflammatory diseases. Animal studies should be additionally conducted in the future to evaluate the potential of DK for treating inflammatory diseases. This study, by verifying the effective anti-inflammatory capabilities of DK, a compound derived from *P. japonicum*, is anticipated to contribute to research into the anti-inflammatory effects of other compounds isolated from *P. japonicum*. Furthermore, this research is expected to serve as a valuable resource for exploring compounds associated with the anti-inflammatory properties inherent to *P. japonicum*.

Data availability statement

Data will be made available on request.

CRediT authorship contribution statement

Ji Hyeon Park: Writing – original draft, Visualization, Investigation, Data curation. **Jang Hoon Kim:** Writing – original draft, Validation, Methodology, Conceptualization. **Seon Il Jang:** Writing – review & editing. **Byoung Ok Cho:** Writing – review & editing, Supervision, Project administration, Methodology, Funding acquisition, Conceptualization.

Declaration of competing interest

The authors declare that they have no known competing financial interests or personal relationships that could have appeared to influence the work reported in this paper.

Acknowledgement

The research presented in this paper was supported by a “Cooperative Research Program for Agriculture Science & Technology Development” (Project No. RS-2022-RD010239) funded by the Rural Development Administration of the Republic of Korea.

Appendix A. Supplementary data

Supplementary data to this article can be found online at https://doi.org/10.1016/j.heliyon.2023.e21032.

References

[1] M. Hisamoto, H. Kikuzaki, H. Ohigashi, N. Nakatani, Antioxidant compounds from the leaves of Peucedanum japonicum thunb, J. Agric. Food Chem. 51 (18) (2003) 5255–5261.
[2] R.-Y. Choi, S.-J. Nam, J.R. Ham, H.-I. Lee, S.-T. Yee, K.-Y. Kang, K.-I. Seo, J.-H. Lee, M.-J. Kim, M.-K. Lee, Anti-adipogenic and anti-diabetic effects of cis-3′, 4′-diisovalerylkhellactone isolated from Peucedanum japonicum Thunb leaves in vitro, Bioorg. Med. Chem. Lett 26 (19) (2016) 4655–4660.
[3] M.H. Do, J.H. Lee, J. Ahn, M.J. Hong, J. Kim, S.Y. Kim, Isosamidin from Peucedanum japonicum roots prevents methylglyoxal-induced glucotoxicity in human umbilical vein endothelial cells via suppression of ROS-mediated bax/bcl-2, Antioxidants 9 (6) (2020).
[4] S.O. Lee, S.Z. Choi, J.H. Lee, S.H. Chung, S.H. Park, H.C. Kang, E.Y. Yang, H.J. Cho, K.R. Lee, Antidiabetic coumarin and cyclitol compounds from Peucedanum japonicum, Arch Pharm. Res. (Seoul) 27 (12) (2004) 1207–1210.
[5] L. Chen, H. Deng, H. Cui, J. Fang, Z. Zuo, J. Deng, Y. Li, X. Wang, L. Zhao, Inflammatory responses and inflammation-associated diseases in organs, Oncotarget 9 (6) (2018) 7204.
[6] J.L. Lai, Y.H. Liu, C. Liu, M.P. Qi, R.N. Liu, X.F. Zhu, Q.G. Zhou, Y.Y. Chen, A.Z. Guo, C.M. Hu, Indirubin inhibits LPS-induced inflammation via TLR4 abrogation mediated by the NF-kB and MAPK signaling pathways, Inflammation 40 (1) (2017) 1–12.
[7] J.M. Han, E.K. Lee, S.Y. Gong, J.K. Sohng, Y.J. Kang, H.J. Jung, Sparassis crispa exerts anti-inflammatory activity via suppression of TLR-mediated NF-κB and MAPK signaling pathways in LPS-induced RAW264. 7 macrophage cells, J. Ethnopharmacol. 231 (2019) 10–18.
[8] J.P. Cooke, Inflammation and its role in regeneration and repair: a caution for novel anti-inflammatory therapies, Circ. Res. 124 (8) (2019) 1166–1168.
[9] N. Tatiya-Aphiradee, W. Chatuphonprasert, K. Jarukamjorn, Immune response and inflammatory pathway of ulcerative colitis, J. Basic Clin. Physiol. Pharmacol. 30 (1) (2018) 1–10.
[10] M.B. Labib, A.M. Fayez, E.-N. EL-Shaymaa, M. Awadallah, P.A. Halim, Novel tetrazole-based selective COX-2 inhibitors: design, synthesis, anti-inflammatory activity, evaluation of PGE2, TNF-α, IL-6 and histopathological study, Bioorg. Chem. 104 (2020), 104308.
[11] S. Singh, D. Anshita, V. Ravichandiran, MCP-1: function, regulation, and involvement in disease, Int. Immunopharm. 101 (2021), 107598.
[12] N. Tripathi, S. Paliwal, S. Sharma, K. Verma, R. Gururani, A. Tiwari, A. Verma, M. Chauhan, A. Singh, D. Kumar, Discovery of novel soluble epoxide hydrolase inhibitors as potent vasodilators, Sci. Rep. 8 (1) (2018), 14604.
[13] W. Zhang, H. Li, H. Dong, J. Liao, B.D. Hammock, G.-Y. Yang, Soluble epoxide hydrolase deficiency inhibits dextran sulfate sodium-induced colitis and carcinogenesis in mice, Anticancer research 33 (12) (2013) 5261–5271.
[14] H. Li, J.A. Bradbury, M.L. Edin, J.P. Graves, A. Gruzdev, J. Cheng, S.L. Hoopes, L.M. DeGraff, M.B. Fessler, S. Garantziotis, sEH promotes macrophage phagocytosis and lung clearance of Streptococcus pneumoniae, J. Clin. Investig. 131 (22) (2021).
[15] J. Zhang, F.-Y. Yang, Q.-M. Zhu, W.-H. Zhang, M. Zhang, J. Yi, Y. Wang, H.-L. Zhang, G.-B. Liang, J.-K. Yan, Inhibition effect of 1-acetoxy-6α-(2-methylbutyryl) eriolanolide toward soluble epoxide hydrolase: multispectral analysis, molecular dynamics simulation, biochemical, and in vitro cell-based studies, Int. J. Biol. Macromol. 235 (2023), 123911.
[16] W.-Y. Zhao, X.-Y. Zhang, M.-R. Zhou, X.-G. Tian, X. Lv, H.-L. Zhang, S. Deng, B.-J. Zhang, C.-P. Sun, X.-C. Ma, Natural soluble epoxide hydrolase inhibitors from Alisma orientale and their potential mechanism with soluble epoxide hydrolase, Int. J. Biol. Macromol. 183 (2021) 811–817.
[17] M. Ramos-Rodríguez, H. Raurell-Vila, M.L. Colli, M.I. Alvelos, M. Subirana-Granés, J. Juan-Mateu, R. Norris, J.-V. Turatsinze, E.S. Nakayasu, B.-J.M. Webb-Robertson, The impact of proinflammatory cytokines on the β-cell regulatory landscape provides insights into the genetics of type 1 diabetes, Nat. Genet. 51 (11) (2019) 1588–1595.
[18] C. Wang, Y. Gao, Z. Zhang, Q. Chi, Y. Liu, L. Yang, K. Xu, Safflower yellow alleviates osteoarthritis and prevents inflammation by inhibiting PGE2 release and regulating NF-κB/SIRT1/AMPK signaling pathways, Phytomedicine 78 (2020), 153305.
[19] T.Y. Gil, B.R. Jin, H.J. An, Peucedanum japonicum Thunberg alleviates atopic dermatitis-like inflammation via STAT/MAPK signaling pathways in vivo and in vitro, Mol. Immunol. 144 (2022) 106–116.
[20] R.J. Pickering, Oxidative Stress and Inflammation in Cardiovascular Diseases, MDPI, 2021, p. 171.
[21] J.H. Kim, J.S. Park, Y.J. Lee, S. Choi, Y.H. Kim, S.Y. Yang, Inhibition of soluble epoxide hydrolase by phytochemical constituents of the root bark of Ulmus davidiana var. japonica, J. Enzym. Inhib. Med. Chem. 36 (1) (2021) 1049–1055.
[22] L. Chen, H. Deng, H. Cui, J. Fang, Z. Zuo, J. Deng, Y. Li, X. Wang, L. Zhao, Inflammatory responses and inflammation-associated diseases in organs, Oncotarget 9 (6) (2018) 7204–7218.
[23] T. Muthumalage, I. Rahman, Cannabidiol differentially regulates basal and LPS-induced inflammatory responses in macrophages, lung epithelial cells, and fibroblasts, Toxicol. Appl. Pharmacol. 382 (2019), 114713.
[24] J. Klauder, J. Henkel, M. Vahrenbrink, A.-S. Wohlenberg, R.G. Camargo, G.P. Püschel, Direct and indirect modulation of LPS-induced cytokine production by insulin in human macrophages, Cytokine 136 (2020), 155241.
[25] E. Moita, A. Gil-Izquierdo, C. Sousa, F. Ferreres, L.R. Silva, P. Valentão, R. Domínguez-Perles, N. Baenas, P.B. Andrade, Integrated analysis of COX-2 and iNOS derived inflammatory mediators in LPS-stimulated RAW macrophages pre-exposed to Echium plantagineum L. bee pollen extract, PLoS One 8 (3) (2013), e59131.
[26] H. Harizi, N. Gualde, Pivotal role of PGE2 and IL-10 in the cross-regulation of dendritic cell-derived inflammatory mediators, Cell. Mol. Immunol. 3 (4) (2006) 271–277.
[27] M.R. Fernando, J.L. Reyes, J. Iannuzzi, G. Leung, D.M. McKay, The pro-inflammatory cytokine, interleukin-6, enhances the polarization of alternatively activated macrophages, PLoS One 9 (4) (2014), e94188.
[28] M. Cuellar-Núñez, E.G. De Mejia, G. Loarca-Piña, Moringa oleifera leaves alleviated inflammation through downregulation of IL-2, IL-6, and TNF-α in a colitis-associated colorectal cancer model, Food Res. Int. 144 (2021), 110318.
[29] F. Asgharpour, A.A. Moghadamnia, M. Motallebnejad, H.R. Nouri, Propolis attenuates lipopolysaccharide-induced inflammatory responses through intracellular ROS and NO levels along with downregulation of IL-1β and IL-6 expressions in murine RAW 264.7 macrophages, J. Food Biochem. 43 (8) (2019), e12926.
[30] W. Tong, X. Chen, X. Song, Y. Chen, R. Jia, Y. Zou, L. Li, L. Yin, C. He, X. Liang, Resveratrol inhibits LPS-induced inflammation through suppressing the signaling cascades of TLR4-NF-κB/MAPKs/IRF3, Exp. Ther. Med. 19 (3) (2020) 1824–1834.
[31] T. Behl, T. Rana, G.H. Alotaibi, M. Shamsuzzaman, M. Naqvi, A. Sehgal, S. Singh, N. Sharma, Y. Almoshari, A.A. Abdellatif, Polyphenols inhibiting MAPK signalling pathway mediated oxidative stress and inflammation in depression, Biomed. Pharmacother. 146 (2022), 112545.
[32] M.Z. Khan, A. Khan, J. Xiao, J. Ma, Y. Ma, T. Chen, D. Shao, Z. Cao, Overview of research development on the role of NF-κB signaling in mastitis, Animals 10 (9) (2020) 1625.
[33] E. Sun, A. Motolani, L. Campos, T. Lu, The pivotal role of NF-kB in the pathogenesis and therapeutics of alzheimer's disease, Int. J. Mol. Sci. 23 (16) (2022).
[34] J. Shen, J. Cheng, S. Zhu, J. Zhao, Q. Ye, Y. Xu, H. Dong, X. Zheng, Regulating effect of baicalin on IKK/IKB/NF-kB signaling pathway and apoptosis-related proteins in rats with ulcerative colitis, Int. Immunopharm. 73 (2019) 193–200.
[35] M.S. Hayden, S. Ghosh, Shared principles in NF-kappaB signaling, Cell 132 (3) (2008) 344–362.